Aalborg Universitet

PAPER • OPEN ACCESS

Validating a Building Performance Simulation Model of a naturally ventilated Double Skin Facade

View the article online for updates and enhancements.

Validating a Building Performance Simulation Model of a naturally ventilated Double Skin Facade

M Schaffer[1*], L A Bugenings[2], O K Larsen[1]

[1] Department of the Built Environment, Aalborg University, Aalborg, 9220, Denmark
[2] Department of Civil and Architectural Engineering, Aarhus University, Aarhus, 8000, Denmark

*Corresponding author: msch@build.aau.dk

Abstract. Double Skin Facades (DSF) are regaining popularity as a way to increase the climate resilience of buildings. Building Performance Simulation (BPS) is commonly used for their assessment, but modelling DSFs with BPS is challenging due to their complex thermophysical behaviour. Several research works have evaluated the capabilities and limitations of BPS for modelling specific DSF configurations. This work presents a validation study based on experimental data from a full-scale naturally ventilated double-skin façade, compared against results from the BPS software IDA-ICE. The study found that in periods with low solar irradiation, the different modelling strategies had a minor influence on the results, with a high agreement between measurements and simulation. In contrast, periods with solar irradiation showed a higher sensitivity to the modelling strategy, with more significant deviations from the measurement results.

1. Introduction

Double Skin Facades (DSF) are regaining popularity in light of the intensifying efforts to increase the climate resilience of existing and new buildings. Their strengths are found within responsive behaviour and use of natural ventilation. Meanwhile, their application remains reliant on the availability of building performance simulation (BPS) software able to support practitioners and researchers in evaluating performance not only of the DSF alone but of the entire building and envelope system. The concept of DSF is not new, but even nowadays, the use of BPS tools for DSF can still be challenging and can result in high-performance uncertainty [1–3]. An adequate performance assessment of the DSF requires a model that considers the airflow path, driving forces, potential integration of solar shading solutions, and control of openings.

This work utilises the empirical test case of [4] IEA Annex 34/43 to validate IDA-ICE software for naturally ventilated DSF and, in this way, to contribute to the overall validation effort in the research community. Previously, leading BPS software such as VA114, ESP-r, TRNSYS-TUD and BSim were validated [2]. Initially, IDA-ICE (version 3.0) was included in that work, but the final modelling iteration could not be carried out, and the final results were never published for the IDA-ICE model. Other validation efforts include the validation of EnergyPlus for naturally and mechanically ventilated DSF [3,5–8] and more recent works targeting several BPS software, including IDA-ICE, for the validation of mechanically ventilated DSF [9]. Two fundamentally different approaches to model DSF are named, (1) as an individual model where the DSF is represented using single or multiple thermal zones and an airflow network or (2) using the, in the software, inbuilt component/routine specifically designed to

model DSF [1]. Meanwhile, the IDA-ICE model sensitivity towards the use of one or the other approach is addressed by a comparative evaluation by [7,10]. In terms of model development, such aspects as the model geometry, e.g., the division of the cavity space into several vertically-stacked thermal zones for better prediction of the vertical temperature gradient (e.g. [4,10,11]), assumptions towards convective heat transfer coefficient (CHTC) in the model (e.g. [1,4,10]), implementation of the glazing optical properties [4], modelling of wind effects [12] and re-emerging difficulties in DSF performance evaluation under high solar exposure are the main topics being addressed.

In this study, we evaluate various modelling strategies for DSF using IDA-ICE version 4.8 SP2 [13] by comparison of the model results with the empirical data set. The research focus is set on three main areas: (1) modelling the DSF cavity as one thermal zone to confirm the coherence of this work with the previous studies, (2) integration of the detailed IDA-ICE window model to account for the specific properties of the glazing, and (3) analysis of the model results with respect to algorithms used for the internal CHTC, as no generally accepted recommendation on this matter could be found, and most CHTC-related decisions in the modelling practice appear experience-based.

2. Methodology

2.1. Experimental characteristics

The full-scale experiment conducted by [4] is outlined in the following. It consists of two sets of data, one for a DSF as a transparent insulation (case DSF100e – 18 days) and one for a DSF as an external air curtain (case DSF200e – 14 days). This study's particularity is the monitoring of the, to the DSF, adjacent room, including the energy consumption for heating and cooling to keep a constant indoor temperature of 21.8 °C. The test facility was located near Aalborg, Denmark. The facility consisted of a south-oriented DSF and an adjacent room (Figure 1).
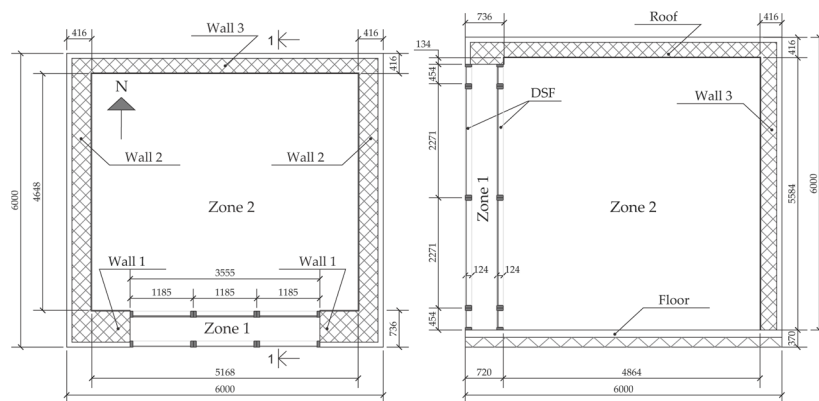
Figure 1. Floorplan (a) and section (b) of the experimental facility, including construction types - redrawn based on [4].

The outer glazing is uncoated single-pane glazing, while the glazing between DSF and the room is double-pane glazing with a low-ε coating on position three. The interested reader is referred to the detailed description in [4] for more details.

2.2. Simulation model characteristics

The BPS model used follows the case study's description by [4]. Thus, only the deviations from the specification and significant aspects are outlined. Each zone of the test facility, including the DSF, was represented by one thermal zone in IDA-ICE.

As only the global horizontal irradiance (GHI) and diffuse horizontal irradiance (DHI) were available, this data was converted to direct normal irradiance (DNI) and DHI for use in IDA-ICE. IDA-ICE uses a power-law wind speed profile; thus, the given logarithmic profile could not be used. A close approximation of the given profile was found with the coefficient of a power-law profile set to 1.05 and the exponent set to 0.4.

The DSF is embedded in the exterior wall and cannot be modelled in IDA-ICE directly. Instead, each sidewall of the cavity was modelled with the construction of the south exterior wall, and the top side was modelled as a roof, all facing exterior. Thermal conditions in the room adjacent to the DSF were maintained by a purely convective ideal cooling and heating system miming the recirculating ventilation system used in the experiment. Increased activation of the thermal mass of the concrete floor due to an omnidirectional supply of air from the textile diffusers placed on the floor of the experiment room was not considered in the model, as no appropriate strategy was found to model this effect. Each window was modelled using the detailed window model of IDA-ICE, as one component, with corresponding frame area. The glazing was defined pane by pane. The provided spectral data could have been directly used in IDA-ICE. However, the implementation is cumbersome and must be done manually. Consequently, the spectral data were processed in Optics, from which all necessary information could be obtained to define the individual windowpanes in IDA-ICE. Thermal brides were given as the difference between measured and calculated transmission losses, expressed as a linear function of the temperature difference. Based on this, the thermal bridge was calculated, and the resulting 0.013 kW/K were evenly distributed over the envelope. Infiltration was calculated with the given data at a pressure difference of 50 Pa and used as input for wind-driven infiltration in IDA-ICE. As the wind pressure coefficients can only be specified per facade in IDA-ICE, the values for the top and bottom were averaged. For the roof, a constant pressure coefficient of 0.1 was defined.

The opening area was set as specified for case DSF200e, where the small top and bottom windows are opened. It is, per default, not possible in IDA-ICE to specify the discharge coefficient depending on the flow direction. Thus, a constant flow direction where the bottom windows serve as supply openings and the top window as exhaust openings was assumed, and the discharge coefficients were set accordingly.

For the room, the, in IDA-ICE available, CHTC algorithm "Simple natural convection" was used since the air velocity of the recirculating ventilation system was consistently below 0.2 m/s. For the DSF, all in IDA-ICE available CHTC algorithms were tested. These are: the BRIS model, Simple Natural Convection (SNC) model, Detailed Natural Convection (DNC) model, Ceiling diffuser (CD) model, BRIS/CD Model and DNC/CD Model. These algorithms can be divided into three groups: temperature difference (T_{air}-T_{srf}) controlled (Bris, SNC and DNC model), air change (ACH) controlled (CD model) and a combination of the two previous where the larger CHTC is selected (BRIS/CD and DNC /CD).

2.3. Result evaluation

Heating and cooling power, the air cavity temperature and the innermost glazing surface temperature ($T_{srf\,ii}$) were used for the evaluation. The heating and cooling power represents the overall heat balance for the room and is a crucial element for evaluation. The air cavity temperature is used to assess the energy balance of the DSF cavity. The innermost glazing temperature was chosen as it represents the interface between DSF and the room and has, thus, e.g., an effect on the thermal comfort (radiation asymmetry). For case DSF200e, the external air curtain DSF, additionally, the mass flow through the DSF was evaluated. Here, it is to be noted that this was measured in two different ways, once with the tracer gas method and once with the velocity profile method. Both measures are subject to specific errors described in detail in [4]. For the mass flow rate based on the velocity profile method, the height of 1.91m was used for evaluation. The results are first presented as a detailed analysis for two days. After that, the performance of each model is analysed for the whole evaluation period based on the normalised root mean square error (NRMSE) defined as the RMSE/absolute mean of the respective measured quantity: Normalising the RMSE by the absolute mean of the respective measured quantity allows for easier evaluation across different quantities and magnitudes and the two tested cases (DSF100e and DSF 200e). The absolute mean was chosen to avoid cancelling opposite signs as the power is measured with positive (heating) and negative (cooling) signs. The NRMSE was calculated for the whole period of each case, 18 days for case DSF100e and 14 days for case DSF200e.

3. Result

The results of the two double-skin ventilation modes, transparent insulation (DSF100e) and external air curtain (DSF200e), are presented in the following. For both cases, two representative days were chosen for the in-depth analysis. The 24th and 25th of October were selected for case DSF100e, and the 10th and 11th of October for DSF200e, as they include a day with low solar irradiation and a day with high solar irradiation. For case DSF200e, the measurement period till the 11th of October was classified as difficult to evaluate in terms of air mass flow rate through the DSF due to external conditions such as strong wind and a highly fluctuating wind direction. Thus, for the mass flow rate, only the period from the 13th to the 14th of October is additionally evaluated as a period with stable wind directions and low wind velocities (<6 m/s).

3.1. Transparent insulation - DSF100e

Figure 2 shows the measured and simulated solar irradiation on the façade, where a good agreement can be seen. Still, a trend of over-prediction is confirmed by a mean deviation of 6.56 W/m^2 for the whole simulation period. Apparent deviations are visible at the forenoon of the 24th and noon of the 25th. The divergence on the 24th can be led back to a possible measurement error of the solar irradiation on the façade. Possible measurement errors could be rain droplets on the pyranometer or changed ground reflectance (e.g., wet surface). Still, it must be considered that the solar model (Perez model) used in IDA-ICE can also cause deviations between simulation and measurement.

Figure 3 shows the heating and cooling power simulated using different CHTC algorithms. The heating power is slightly under-predicted in periods with no solar irradiation (night). The period with little solar irradiation shows a distinctive peak in the measured heating power caused by the control system. Excluding this peak, the prediction follows the experimental data well and shows similar behaviour during periods without solar irradiation. In contrast, the simulations show a significant difference in the pattern on the 25th when the direct solar radiation is high. Here, all algorithms show a delay of approximately one hour. The impact of this failure to predict the cooling power correctly continues into the night, where the underprediction of the heating power is more significant compared to the period between the 24th and 25th.
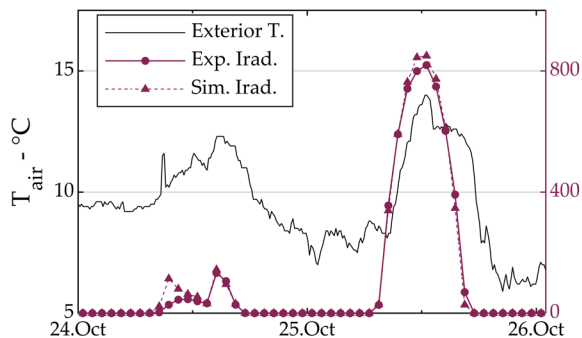
Figure 2. Exterior temperature and comparison of measured and simulated solar irradiation on the DSF for case DSF100e
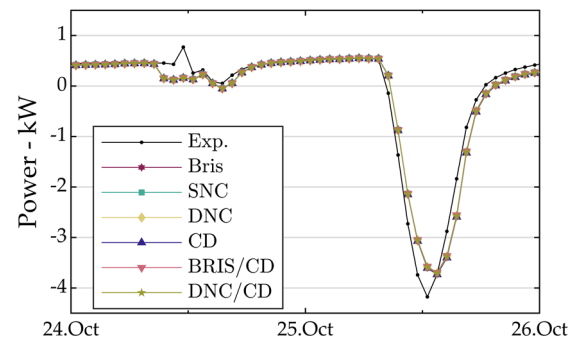

Figure 3. Heating (positive) and cooling (negative) power for the different CHTC algorithms for case DSF100e

A tendency to slightly underpredict the cavity temperature and only minor deviation between the different algorithms during the absence of solar irradiation is seen for all algorithms (Figure 4). The trend of an overpredicted cavity temperature is seen for the daytime of the 24th, primarily in the period when calculated and measured solar irradiance do not match. However, the disagreement is more evident for the daytime of the 25th. Here, also the difference between the CHTC algorithms is notable, where those that are temperature-difference dependent, and the combined algorithms differ from the ventilation-rate based algorithm (CD). The CD algorithm leads thereby to a lower cavity air temperature. Another relevant aspect to consider is the temperature profile at the beginning and end of the day. The general observation here is that the temperature rise in the model is underestimated, and the rate of the

temperature drop is overestimated. The higher rate of thermal mass activation in the cavity (i.e. concrete floor) also appears to be characteristic for the CD algorithm.

Similar trends are seen for the interior glazing surface temperature, $T_{srf\,ii}$ (Figure 5). The deviation at the end of the second day is less compared to the cavity air temperature. The algorithms show hardly any difference.
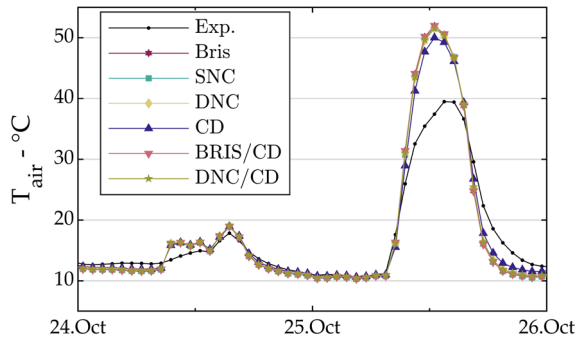
Figure 4. Volume averaged T_{air} of the DSF for the different algorithms for case DSF100e
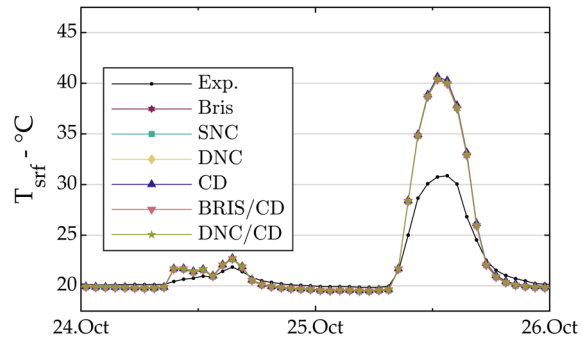
Figure 5. Area averaged $T_{srf\,ii}$ for the different algorithms for case DSF100e

For this first analysis of the two selected days, it can be concluded that all models predict periods without (intense) solar irradiation better than periods with solar irradiation, where the deviation is significant and can reach about 50 %. In periods with solar irradiation, the cooling demand tends to be smaller or equal to the measurement and shifted by about one hour, while the air temperature of the DSF and the inner glazing surface temperature are far too high in the model. Overall, the different CHTC algorithms show little influence on the results. These results could also be confirmed by analysing the NRMSE for the whole period of case DSF100e (Table 1).

Table 1. NRMSE based on the whole period of case DSF100e. Day and night were separated based on the measured solar irradiation on the façade ($\leq 5W/m^2$).

|	NRMSE								
	Inner glazing surface temperature			DSF air temperature			Heating and cooling power		
	day	night	total	day	night	total	day	night	total
BRIS	0.128	0.021	0.084	0.270	0.098	0.208	0.472	0.186	0.392
SNC	0.129	0.023	0.085	0.268	0.099	0.207	0.471	0.179	0.390
DNC	0.131	0.019	0.085	0.264	0.092	0.203	0.475	0.196	0.397
CD	0.133	0.017	0.087	0.241	0.072	0.183	0.477	0.204	0.400
BRIS/CD	0.129	0.021	0.084	0.272	0.098	0.209	0.472	0.186	0.392
DNC/CD	0.131	0.019	0.085	0.265	0.092	0.203	0.475	0.196	0.397

3.2. External air curtain - DSF200e

Figure 6, showing the measured and simulated solar irradiation of the façade for case DSF200e, shows a clear time shift on the 10th and a slight over-prediction of the peak. The reason for this time shift could not be determined as the same approach as for case DSF100e was used, and the shift did not appear uniformly on every day of the calculation period. Additionally, the trend of over-prediction over the whole simulated period is shown by a positive mean deviation of 0.72 W/m². The measurement and simulation agree well for the second day. The heating and cooling power (Figure 7) overall show a similar trend as for the transparent insulation mode. In periods without solar irradiation, the variance between the different algorithms is small, and the heating power is repeatedly predicted as too low. For the more significant peak on the 10th, a time shift of about one hour for the cooling power peak can be seen for all algorithms. Partly the reason for this could be the shift already seen for the simulation's solar irradiation on the DSF. Further, the variance between the different algorithms increases strongly with

increasing solar irradiation. Here, all algorithms are either controlled only by ACH (CD) or by the temperature difference, and ACH (BRIS/CD and DNC/CD) show a lower cooling power than those only controlled by temperature. This failure to correctly predict the peak also leads to a more substantial underestimation of the heating power till the next morning.
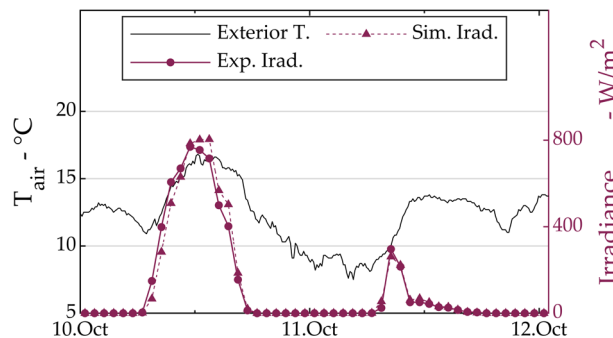
Figure 6. Exterior temperature and comparison of measured and simulated solar irradiation on the DSF for case DSF200e
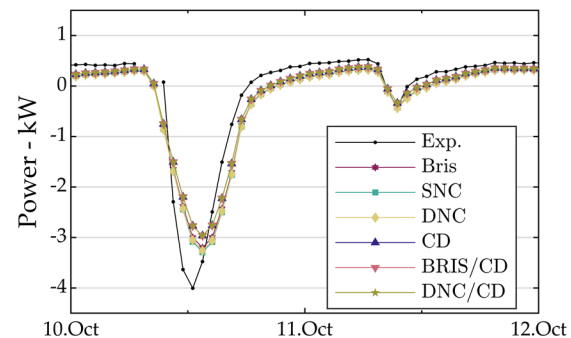
Figure 7. Heating (positive) and cooling (negative) power for the different CHTC algorithms for case DSF200e

The most significant result for the air temperature in the cavity (Figure 8 a)) is that the difference between different algorithms is almost zero for all periods without solar irradiation. At periods with solar irradiation, the variance increases to about 4 °C in peak on the 10th. The ACH-controlled and combined algorithms show a too-high cavity temperature, whereas the sole temperature-controlled algorithms underpredict the cavity temperature. Still, the results show a much better agreement with the measured cavity temperature than for the transparent insulation mode, even in periods with high solar irradiation. Only in the first two hours of the temperature rise on the 10th all algorithms strongly underestimate the temperature rise.

The results for the innermost glazing surface temperature (Figure 8 b)) show a good agreement with the experimental data and a similar pattern as the air temperature in the DSF for periods without solar irradiation. However, the surface temperature is greatly overpredicted during periods with high solar irradiation. The variance between the different CHTC algorithms increases with increasing solar irradiation. Sole temperature-controlled algorithms, BRIS, SNC and DNC, show thereby higher temperatures than the remaining algorithms. During the temperature decrease after the peak on the 10th, all algorithms predict the decline too late, leading to too high surface temperatures and, thus, higher error compared to the temperature rise period on the same day.

The last criterion evaluated is the mass flow rate. For the period between the 10th and 11th of October, the results show a slight variance for different CHTC algorithms during the period with no solar irradiation and an increasing variation with increasing solar irradiation (Figure 8 c)). Overall, a good agreement with the experiment results around noon and early afternoon on the 10th is shown. During the night period between the 10th and 11th, the simulation predicts about 50 kg/h to 100 kg/h too high mass flow and shows a more stable flow than the experiment. On the 11th, all models fail to predict the increase in the flow during the day. For all other periods, there is no correlation between measurement and experiment visible.

For the second analysed period, Figure 8 d) shows the same trend as the measurement with an overall magnitude between the tracer-gas and velocity profile measurements results. Again, the variance between different CHTC algorithms increases with rising solar irradiation. For both periods, the sole temperature difference-driven algorithms generally lead to a lower mass-flow rate under solar irradiation.

For this second analysis, it can be concluded that all models predict periods without (intense) solar irradiation better than periods with solar irradiation. The cooling power is again greatly underpredicted and shows a clear shift to the measurement when the solar irradiation is high. At the same time, the inner glazing surface temperature is significantly too high, while the DSF air temperature is predicted

correctly. Principal agreement with the measurements could be observed for the mass flow rate. The different CHTC algorithms show apparent differences in period with a high-volume flow, as the high ACH in the DSF cavity leads to a significant difference between ACH and temperature difference-driven algorithm. However, overall, no superior could be identified. The NRMSE could again confirm these results for the whole period of case DSF200e (Table 2).
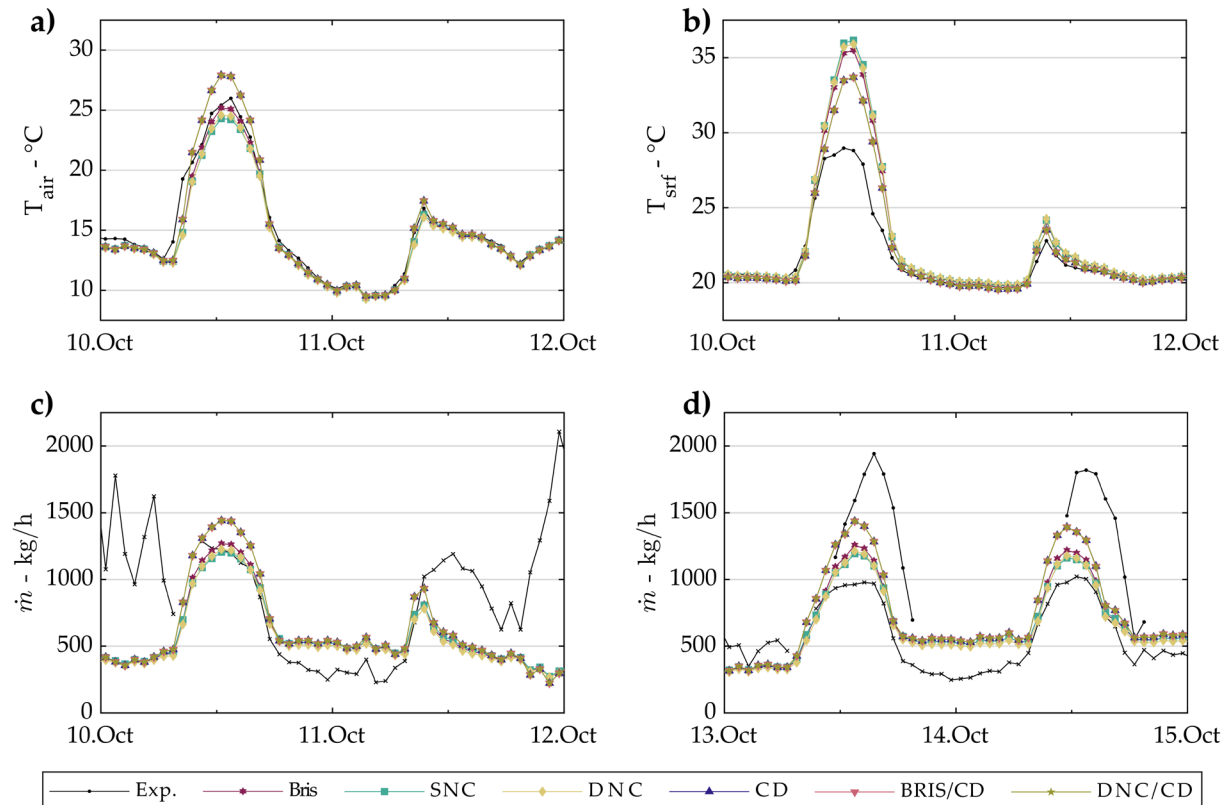
Figure 8 a) Volume averaged T_{air} of the DSF **b)** Area averaged $T_{srf\ ii}$ **c)** Mass flow rate through the DSF. **d)** Mass flow rate through the DSF for two additional selected days – all for case DSF200e.

Table 2 NRMSE based on the whole period of case DSF200e. Day and night were separated based on the measured solar irradiation on the façade ($\leq 5W/m^2$)

	NRMSE								
	Inner glazing surface temperature			DSF air temperature			Heating and cooling power		
	day	night	total	day	night	total	day	night	total
BRIS	0.119	0.008	0.085	0.055	0.039	0.051	0.468	0.505	0.516
SNC	0.128	0.008	0.092	0.056	0.038	0.051	0.468	0.504	0.516
DNC	0.127	0.010	0.091	0.057	0.043	0.053	0.470	0.527	0.522
CD	0.082	0.010	0.059	0.098	0.037	0.082	0.479	0.409	0.506
BRIS/CD	0.082	0.010	0.059	0.098	0.037	0.082	0.479	0.409	0.506
DNC/CD	0.082	0.010	0.059	0.098	0.037	0.082	0.479	0.409	0.506

4. Discussion and conclusion

This study validated an IDA-ICE model for a naturally ventilated DSF in two states, as transparent insulation (case DSF100e) and as an external air curtain (case DSF200e). Additionally, different CHTC algorithms were investigated for the DSF. Overall, regarding the CHTC algorithms, for case DSF100e, only minor influence could be seen, while the influence for case DSF200e was more considerable, and

no superior algorithm could be identified. Furthermore, the results demonstrate that the model's accuracy decreases drastically in periods with high solar irradiation.

For both cases, the cooling power exhibited a shift and was underestimated in periods with high solar irradiation. While further investigations are necessary to determine the cause for this with certainty, it is seen as likely that this is interlinked with the definition and activation of thermal mass in the BPS model. In contrast, the interior glazing surface temperature was greatly overpredicted in the presence of solar irradiation, indicating that the heat transfer from the DSF to the adjunct room could be mispredicted. Similar results could be seen for case DSF100e for the DSF air temperature, while a good agreement could be seen for case DSF200e, even in the presence of solar irradiation. Also, the air mass flow rate through the DSF in case DSF200e shows a good agreement with the measurement.

In conclusion, the model shows a high agreement with the measurements in periods without or with low solar irradiation, while in periods with high solar irradiation, significant deviations are observed. Regarding the investigated CHTC algorithms, no superior algorithm could be determined.

References

[1]   Catto Lucchino E, Goia F, Lobaccaro G and Chaudhary G 2019 Modelling of double skin facades in whole-building energy simulation tools: A review of current practices and possibilities for future developments Building Simulation **12**:1 3–27

[2]   Kalyanova O, Heiselberg P, Felsmann C, Poirazis H, Strachan P and Wijsman A 2009 *Building Simulation 2009: Proc. of the 11th Int. Building Performance Simulation Association Conf.* (Glasgow) ed Paul A. Strachan, Nick J. Kelly, Michaël Kummert An Empirical Validation of Building Simulation Software for Modelling of Double-Skin Facade (DSF) pp 1107-14

[3]   Kim D W and Park C S 2011 Difficulties and limitations in performance simulation of a double skin façade with EnergyPlus Energy Build **43** 3635–45

[4]   Kalyanova O and Heiselberg P 2008 Empirical Validation of Building Simulation Software : Modeling of Double Facades

[5]   Mateus N M, Pinto A and Graça G C da 2014 Validation of EnergyPlus thermal simulation of a double skin naturally and mechanically ventilated test cell Energy Build **75** 511–22

[6]   el Ahmar S, Battista F and Fioravanti A 2019 Simulation of the thermal performance of a geometrically complex Double-Skin Facade for hot climates: EnergyPlus vs. OpenFOAM Building Simulation **12**:5 781–95

[7]   Gelesz A, Catto Lucchino E, Goia F, Serra V and Reith A 2020 Characteristics that matter in a climate façade: A sensitivity analysis with building energy simulation tools Energy Build **229** 110467

[8]   Gelesz A, Catto Lucchino E, Goia F, Reith A and Serra V 2019 *Proc. of Building Simulation 2019: 16th Conf. of IBPSA* Reliability and Sensitivity of Building Performance Simulation Tools in Simulating Mechanically Ventilated Double Skin Façades

[9]   Catto Lucchino E, Gelesz A, Skeie K, Gennaro G, Reith A, Serra V and Goia F 2021 Modelling double skin façades (DSFs) in whole-building energy simulation tools: Validation and inter-software comparison of a mechanically ventilated single-story DSF Build Environ **199** 107906

[10]   Gelesz A 2019 Sensitivity of exhaust-air façade performance prediction to modelling approaches in IDA ICE International Review of Applied Sciences and Engineering **10** 241–52

[11]   Saelens D 2002 Energy Performance Assessment of Single Storey Multiple-Skin Facades. PhD Thesis. (Leuven)

[12]   Dama A, Angeli D and Larsen O K 2017 Naturally ventilated double-skin façade in modeling and experiments Energy Build **144** 17–29

[13]   EQUA Simulation AB 2020 IDA-ICE - IDA Indoor Climate and Energy